



Published in final edited form as:

Leukemia. 2021 July ; 35(7): 1990–2001. doi:10.1038/s41375-020-01105-0.

Regulation of PD-L1 expression is a novel facet of cyclic-AMP-mediated immunosuppression

Binu Sasi¹, Purushoth Ethiraj¹, Jamie Myers¹, An-Ping Lin¹, Shoulei Jiang¹, Zhijun Qiu¹, Kenneth N. Holder², Ricardo C. T. Aguiar^{1,3,*}

¹Division of Hematology and Medical Oncology, Department of Medicine, University of Texas Health Science Center San Antonio, San Antonio, Texas, 78229, USA.

²Department of Pathology, University of Texas Health Science Center San Antonio, San Antonio, Texas, 78229, USA.

³South Texas Veterans Health Care System, Audie Murphy VA Hospital, San Antonio, Texas, 78229, USA.

Abstract

Cyclic-AMP (cAMP) exerts suppressive effects in the innate and adaptive immune system. The PD-1/PD-L1 immune checkpoint down-regulates T-cell activity. Here, we examined if these two immunosuppressive nodes intersect. Using normal and malignant lymphocytes from humans, and the phosphodiesterase 4b (Pde4b) knockout mouse, we found that cAMP induces *PD-L1* transcription and protein expression. Mechanistically, we discovered that the cAMP effectors PKA and CREB induce the transcription/secretion of IL-10, IL-8 and IL-6, which initiate an autocrine loop that activates the JAK/STAT pathway and ultimately increase PD-L1 expression in the cell surface. This signaling axis is disarmed at two specific nodes in subsets of diffuse large B cell lymphoma, which may help explain the variable PD-L1 expression in these tumors. In vivo, we found that despite its immunosuppressive attributes, the PDE4 inhibitor roflumilast did not decrease the clinical activity of checkpoint inhibitors, an important clinical observation given the approved use of these agents in multiple diseases. In summary, we discovered that PD-L1 induction is a part of the repertoire of immunosuppressive actions mediated by cAMP, defined a cytokine-mediated autocrine loop that executes this action and, reassuringly, showed that PDE4 inhibition does not antagonize immune checkpoint blockade in an in vivo syngeneic lymphoma model.

Users may view, print, copy, and download text and data-mine the content in such documents, for the purposes of academic research, subject always to the full Conditions of use:http://www.nature.com/authors/editorial_policies/license.html#terms

*Correspondence to: Ricardo Aguiar, Department of Medicine, UT Health Science Center San Antonio, Phone: 210-567-4860, aguiarr@uthscsa.edu.

Authors' contributions: BS designed, performed and interpreted assays; PE, JM, A-PL, performed and interpreted experiments; SJ and ZQ provided support for in vivo assays; KNH, procured and characterized primary tumors; RCTA conceived the project, designed and interpreted assays, wrote manuscript, which was reviewed and approved by all authors.

Declaration of interests: The authors declare no competing financial interests.

Introduction:

Cyclic-AMP (cAMP) is a broadly acting second messenger that relays extra-cellular signals in a cell type and context specific manner. Through binding to effectors, notably PKA (protein kinase A), elevation of intra-cellular cAMP leads to rapid post-translational modifications in the cytosol, and architectural changes in discrete cellular membrane microdomains. In addition, primarily via the PKA-mediated phosphorylation of CREB (cAMP response element-binding protein), cAMP elicits specific gene transcription programs¹.

In cells of the innate and adaptive immune system, cAMP exerts suppressive effects^{2, 3}. In B and T lymphocytes, sustained elevation of cAMP counters the B-cell receptor (BCR) and T-cell receptor (TCR) function, respectively, at least in part by suppressing the activity of downstream kinases⁴⁻⁸. In addition, cAMP provides tonic negative constraint on the synthesis and secretion of proinflammatory cytokines in monocytes and neutrophils, and limits the LPS-driven stimulation of innate immune response^{2, 3}. Adenylate cyclases produce most of the cellular cAMP¹. In turn, a superfamily of enzymes, the phosphodiesterases (PDE), hydrolyze cAMP into inert 5' AMP and terminates signaling. In cells of the immune system, the PDE4 family accounts for most of the cAMP hydrolysis⁹. This feature, alongside a catalytic structure amenable for specific small molecule-based inhibition, has led to the development and FDA-approval of PDE4 inhibitors as anti-inflammatory and immunosuppressive agents². Further, in part due to cAMP's role in suppressing the BCR, these agents are also being tested for the treatment of mature B cell malignancies¹⁰⁻¹².

Antigen-specific T lymphocytes can recognize and eliminate aberrant cells, including cancer cells. Alongside this capability, a system of immune checkpoints has evolved to regulate the quantity and activity of T cells, thus establishing peripheral tolerance and limiting overt tissue damage. A prominent immune checkpoint system is executed by the PD-1- (programmed cell death protein 1)-PD-L1/2 (programmed cell death protein ligand 1/2) interaction¹³. PD-1, a co-inhibitory receptor expressed on the surface of antigen-stimulated T- cells, interacts ligands PD-L1 and PD-L2. This engagement inhibits T-cell proliferation, survival, cytokine production, and other effector functions¹³. Cancer cells hijack this system by expressing PD-L1 on their surface, binding to cognate PD-1 in activated T-cells, thus foiling anti-cancer immunity, which can be successfully reengaged with checkpoint inhibitors, primarily anti-PD1 and anti-PD-L1 antibodies¹⁴. Considering the role of PD-L1 in halting anti-cancer T-cell activity, significant effort has been placed in identifying regulators of PD-L1 expression. Oncogenes and tumor suppressors, as well as pro-inflammatory cytokines, e.g., IFN- γ , have been shown to induce PD-L1 expression, aiding biomarker identification towards improved therapeutic usage¹⁵.

A putative role for cAMP on PD-L1 expression has not yet been directly examined. An interplay between two broadly immunosuppressive nodes - the cAMP signaling pathway and the PD-1/PD-L1/2 immune checkpoint - is predictable and it would be consistent with cAMP's role as a mediator of inputs that suppress T-cells⁴. Testing this possibility is important as it may unveil a novel regulatory axis that modulates PD-L1 expression and

immune checkpoint function. In addition, this knowledge will advance our understanding of the mechanism of action of FDA-approved PDE4 inhibitors, and may guide decisions on their use in approved^{16–22} and in investigational¹² settings.

Methods:

Detailed materials and methods are provided as supplemental data.

Cell lines and primary tumor samples.

DLBCL cell lines were cultured as reported²³; the DLBCL PDX models have been characterized earlier²⁴, and herein were analyzed ex vivo. De-identified primary human lymph nodes were obtained from the Department of Pathology²⁵, and their use was approved by the Institutional Review Board of the UTHSCSA. All patients signed a consent form.

Mice.

The Pde4b knockout mouse was reported before²⁶. To generate murine B-cell lymphoma models, A20 cells were inoculated subcutaneously in Balb/c mice^{27, 28}. Mice were treated with roflumilast (5mg/kg) or vehicle control (PBS/DMSO), administered daily intraperitoneally (IP), and/or with anti-mouse PD-L1 (clone 10F.9G2) or rat IgG2b isotype control, administered IP (200µg per injection) at 2–3 days intervals. Studies were approved by the Institutional Animal Care and Use Committee of UTHSCSA.

Fluorescence-activated cell sorting (FACS) analysis.

Used to detect PD-L1 in human and murine cells, and to characterize immune cell subpopulations in the mouse. Cells were acquired using a BD FACSCelesta (BD Bioscience) or with a Cytex Aurora (Cytex BioSciences). Data were analyzed with FlowJo software v10.6.2 (FlowJo LLC), as we described²⁹.

Immunoblotting analysis.

Performed to detect PD-L1, pSTAT3 (Y705) pSTAT1 (Y701), pCREB (S133) in human and murine cells, as described³⁰.

RNA isolation, cDNA synthesis and q-RT-PCR.

RNA was isolated and cDNA synthesized from primary human lymph nodes, murine splenocytes, DLBCL cell lines and PDX models, as we described³¹. Q-RT-PCRs were performed as reported³², and gene expression calculated using the 2^{-Ct} method³³. Oligonucleotide sequences are listed in Supplemental Table1.

Chemokine array profiling and cytokine quantification.

DLBCL cells were treated with DMSO or forskolin (40 µM) for 8h and supernatant used for the screening of 105 cytokines/chemokines (Human XL Cytokine Array Kit, R&D Systems), or for the direct detection of IL-10, IL-8 and IL-6.

Luciferase Reporter Assay.

A *PD-L1* promoter reporter construct (pGL3-PD-L1-3kb) was described before³⁴, and luciferase and beta-galactosidase quantified as we reported³⁵.

Statistical analysis.

Performed with the GraphPad Prism 8 software. *P* value < 0.05 was considered significant

Results:

Cyclic-AMP induces PD-L1 expression in DLBCL cell lines.

We used forskolin, an adenylyl-cyclase activator, to increase cAMP levels in DLBCL cell lines and well-characterized DLBCL PDX models analyzed *ex vivo*²⁴, and measured PD-L1 expression using FACS. In all ABC (activated B-cell)-like DLBCL models, we detected a significant increase in PD-L1 expression in the cell surface (mean increase 2.2-fold, range 1.5 to 4.1) in association with higher cAMP levels (Fig. 1A and S1A–B). Conversely, no PD-L1 expression, or increase, was detected in GCB (germinal center B-cell)-like DLBCL cell lines or PDXs, even though cAMP was readily elevated and PKA activated in these models (Fig. S1C–F). Using q-RT-PCR, we determined that cAMP induces *PD-L1* expression at RNA level (Fig. 1B), and with western blot (WB) we found that an increase in PD-L1 expression could also be detected in whole cell lysates (Fig. 1C). To validate the concept that forskolin effects are mediated by cAMP, we used the synthetic, cell-permeable, 8-Bromo-cAMP molecule and recapitulated the induction of PD-L1 expression detected with forskolin (Fig. 1D). In addition, blocking PKA activity with its inhibitor H-89, abrogated cAMP effects, establishing PKA as the effector of cAMP-induced PD-L1 expression (Fig. 1E). We concluded that cAMP, in a PKA-dependent manner, induces PD-L1 transcription and protein expression in subsets of DLBCL.

Modulation of PD-L1 expression by the cAMP-PDE4 axis *in vivo*.

Of the members of the PDE4 family, PDE4B is a prominent regulator of cAMP levels in lymphocytes^{36, 37}. Thus, we used a *Pde4b* knockout (KO) mouse model to test the effects of this enzyme on the expression of PD-L1 in murine B- and T-cells. We collected spleens from 8 to 16-week old, sex matched, *Pde4b* WT or KO mice (n=10) and used FACS to examine surface PD-L1 expression in CD19+ and CD3+ subpopulations. The percentage of B and T-cells expressing PD-L1 was significantly higher in *Pde4b* KO mice than in WT littermates (Fig. 2A); WB of total splenocytes confirmed higher expression of PD-L1 in *Pde4b* KO cells (Fig. 2B). To expand on the DLBCL models and mouse data, we examined the interplay between cAMP/PDE4 signals and PD-L1 expression in freshly obtained primary human specimens, including reactive lymph nodes and B-cell lymphomas. We found that *ex vivo* activation of cAMP signals with forskolin, in combination with the FDA-approved PDE4 inhibitor roflumilast, induced PD-L1 expression at RNA and protein levels (Fig. 2C); unfortunately, additional materials were not available for FACS analysis, but the correlation between WB and FACS data in DLBCL cell lines/PDX and *Pde4b* KO models (Fig. 1A, 1C, 2A–B), indicate that in these primary samples PD-L1 expression increased in the cell surface as well. We concluded that genetic and pharmacological modulation of the cAMP-PDE4B

axis influences PD-L1 expression in untransformed murine B and T lymphocytes and in primary human reactive B cells and lymphomas.

Secreted factor(s) mediate cAMP effects on PD-L1 expression.

PKA phosphorylates and activates the transcription factor CREB (cAMP-response element binding protein), which binds to cAMP response elements (CRE) in promoters of its target genes, and induces transcription¹. Thus, to explore the mechanism(s) by which cAMP induces PD-L1 transcription/expression, we first investigated if through PKA/CREB, cAMP could directly modulate *PD-L1* transcription. Using the “regulatory function” of the UCSC browser and Ensembl, as we reported before³⁵, and the ConSite web interface for prediction of regulatory elements³⁸, we mapped five putative CRE sites to the well-characterized *PD-L1* promoter³⁴ (Fig. S2). Next, using a luciferase reporter construct, we found that elevation of intracellular cAMP readily phosphorylated CREB, but it did not induce reporter activity; conversely, IFN γ , used here as a positive control for *PD-L1* promoter activity, consistently increased luciferase levels (Fig. S2). We concluded that *PD-L1* promoter is not responsive to cAMP and that the putative CRE sites are non-functional.

The JAK/STAT pathway is central to the regulation of PD-L1 expression^{15, 39}. Therefore, we asked whether this signaling module could be involved in the cAMP/PDE4-mediated induction of PD-L1. In DLBCL cell lines and PDX models, elevation of cAMP levels resulted in pronounced STAT3 phosphorylation, and pSTAT3 was also higher in the spleen of Pde4b KO vs. WT mice (Fig. 3A–B). Confirming the participation of JAK signals in this process, we showed that a pan-JAK inhibitor blunted induction of PD-L1 (Fig. 3C). As the JAK/STAT signaling pathway is an important transducer of extracellular stimuli, we postulated that cAMP might promote the secretion of “factor(s)”, which in an autocrine fashion could activate JAK/STAT and induce PD-L1 expression. In support to this hypothesis, we found that the conditioned media from DLBCL cells with transient elevation of cAMP, but not from isogenic models with low cAMP, induced PD-L1 expression and STAT3 phosphorylation (Fig. 3D). We concluded that cAMP promotes the secretion of extra-cellular factors, which likely via an autocrine loop mediated by the JAK-STAT pathway, induce PD-L1 expression.

Cyclic-AMP induces the expression and secretion of multiple cytokines that increase PD-L1 levels.

Part of cAMP’s suppressive effects on the immune system is mediated by cytokines². Thus, we investigated if cytokines could function as intermediaries in the cAMP-driven, JAK/STAT mediated, induction of PD-L1. First, we utilized a protein array to profile the pattern of cytokine secretion in isogenic DLBCL cells in low vs. high cAMP status. In this screening strategy, focusing on cytokines that displayed significant basal signal intensity, reflective of their abundance, and which changed between the two tested conditions, we found that the secretion of IL-10, IL-8 and IL-6 were induced by cAMP (5.7, 1.5 and 1.6 fold increase, respectively, Fig. 4A). We validated this observation by directly quantifying the secretion of each of these cytokines in an extended panel of DLBCL models (Fig. 4B). We also determined that the induction of *IL-10*, *IL-8* and *IL-6* occurs at RNA level, and it is PKA-activity dependent (Fig. S3A–B). In addition, we detected the cAMP-mediated

induction of cytokines transcription in primary human lymphoid tissues, and in normal murine lymphocytes using either a combination of forskolin and roflumilast, or synthetic cell-permeable 8-Br-cAMP (Fig. 4C–D). Next, we showed that recombinant IL-10, IL-8 and IL-6 recapitulated the effects of cAMP on PD-L1 expression (Fig. 4E) and confirmed that cytokine-mediated signaling can activate the PD-L1 promoter (Fig. S3C). Then, to firmly link cAMP to the cytokines-mediated autocrine loop and subsequent PD-L1 induction, we used blocking antibodies directed at IL-10 and IL-6 and/or their receptors, as well as against the IL-8 receptor, CXCR2. Confirming the contributions of all cytokines examined as mediators of cAMP effect, blockade of each individual signal node, significantly blunted cAMP-mediated PD-L1 induction (Fig. 4F). Notably, in GCB-DLBCL cell models, although cAMP activated PKA/CREB (Fig. S1F), it did not induce cytokines expression/secretion to the levels found in ABC-DLBCL (which on average was three orders of magnitude higher in ABC-DLBCL than GCB-DLBCL models), nor it activated the JAK/STAT signals (Fig. S3D–E). Interestingly, although IFN γ engaged the JAK/STAT pathway in GCB-DLBCL models, it also did not upregulate PD-L1 (Fig. S3F). These data suggest that in GCB-type DLBCLs, lymphoma cell intrinsic defects in multiple signaling nodes (i.e., cAMP/cytokine secretion axis, and JAK-STAT activation/PD-L1 promoter transcription module) contribute to the lack of PD-L1 expression. Lastly, we explored public datasets, including cohorts of epithelial tumors, such as melanoma, colon and lung cancer, and DLBCL, and found a significant correlation between *PD-L1* levels and expression of *IL-10*, *IL-8* and *IL-6* and/or their receptors (Fig. S3F). We concluded that cAMP in a PKA-dependent manner drives the expression of multiple cytokines, which initiates an autocrine loop that activates the JAK/STAT pathway and induces PD-L1 expression.

PDE4 blockade does not limit the activity of immune checkpoint inhibitors in a syngeneic murine model of B-cell lymphoma.

Given their broad anti-inflammatory and immunosuppressive effects, PDE4 inhibitors are FDA-approved for the treatment of chronic obstructive pulmonary disease (COPD) (roflumilast) and psoriatic arthritis (apremilast)^{19, 21}. These observations raised the possibility that the suppressive effects on cells on the innate and adaptive immune system, may cause pharmacological inactivation of PDE4 to abrogate the activity of immune checkpoint inhibitors in vivo. To examine this possibility, we developed a syngeneic A20 murine B cell lymphoma model in Balb/c mice (n=60, three cohorts of 20 mice). Importantly, differently from human DLBCL cell lines^{6–8}, the growth of A20 cells are not inhibited by roflumilast (Fig. S4A), thus allowing for a better understating of the role the tumor immune microenvironment in the therapeutic response. Following tumor engraftment, mice were randomized into four treatment arms (n=15 mice/arm) to receive vehicle control (DMSO and isotype antibody), roflumilast (5mg/kg/day IP), anti-PD-L1 (200 μ g IP, 5 doses, alternating every 2–3 days), as described⁴⁰, or the combination of roflumilast and anti-PD-L1. Tumors grew unencumbered in the control and roflumilast-only groups but were similarly and significantly suppressed in the anti-PD-L1 or roflumilast/anti-PD-L1 arms (Fig. 5A), suggesting that the PDE4 inhibitor-mediated immunosuppression does not abrogate the beneficial anti-lymphoma effects of immune checkpoint inhibitors in this model. This difference in tumor growth translated in improved survival for the mice in the anti-PD-L1 or roflumilast/anti-PD-L1 arms (Fig. S4B). To better understand the pattern of

response obtained in these assays, and to define how PDE4 inhibition may influence anti-cancer immune response, we used FACS to examine the tumor microenvironment. The growth inhibition detected in the anti-PD-L1 arm was, expectedly, closely associated with a significant increase in CD3⁺ cells in the tumor milieu (Fig. 5B), which has been previously shown to directly account for these effects⁴⁰. In addition, as predicted given its role in suppressing TCR-signal and T-cell survival, the CD3⁺ T-cells infiltrate was significantly smaller in roflumilast-only treated mice (Fig. 5B). Remarkably, despite their similar clinical response, the tumors of mice in the combination arm (roflumilast + anti-PD-L1) had a significantly less pronounced T-cell infiltrate than the anti-PD-L1 only group (Fig. 5B). To investigate the potential reasons for this intriguing observation, we characterized the CD4/CD8 subpopulations in the tumor microenvironment. Curiously, PDE4 inhibition with roflumilast (as single agent or in combination with anti-PD-L1), increased the proportions of cytotoxic CD8⁺ T-cells and decrease the CD4⁺ T-cell infiltrate and, consequently, decreased the CD4/CD8 ratio (Fig. 5C, Fig. S4B–C), a profile suggested to associate with improved outcome in cancer⁴¹. Surely, in isolation this qualitatively distinct tumor infiltrating lymphocyte (TIL) profile was not sufficient to suppress tumor growth, as lymphomas grew unimpeded in the roflumilast-only arm (Fig. 5A). However, this TIL profile may help explain how even with significantly fewer infiltrating T-cells, the tumors in the combination arm responded similarly to those treated with anti-PD-L1 only (Fig. 5A). Lastly, even though the A20 cell model constitutively express high PD-L1 levels, in accordance with data from normal and malignant human and murine lymphocytes, we detected a modest but significant additional increase in the expression of PD-L1 in the surface of the murine A20 lymphomas in vivo (Fig. S4D). Still, this finding likely has little clinical impact since roflumilast led to a decrease in T-cell infiltration in the microenvironment. We concluded that despite its broad immunosuppressive attributes, the PDE4 inhibitor roflumilast did not decrease the clinical activity of checkpoint inhibitors in a mouse model of B-cell lymphoma. In this model, PDE4 inhibition led to the emergence of a favorable anti-tumor immune profiles including a relative increase in CD8⁺ cytotoxic T-cells.

Discussion:

We discovered that the second messenger cAMP modulates PD-L1 expression and defined the mechanistic basis for this action. Cyclic-AMP is a well-established suppressor of innate and adaptive immune cells^{2, 4}. To date, these effects have been mainly associated with cAMP's ability to dampen the synthesis of pro-inflammatory cytokines by neutrophils and monocytes, and to “tone-down” BCR and TCR function^{2–4, 12}. Our data suggest that induction of PD-L1 expression, with potential engagement of PD-1/PD-L1 pathway and inhibition of cytotoxic T-cells activity, is an additional mechanism by which cAMP executes immunosuppression.

We identified an elaborate autocrine loop as the mechanistic basis for the cAMP/PD-L1 interplay. In human and murine, normal and malignant, lymphocytes, cAMP induces the expression and secretion of the IL-10, IL-8, IL-6, which activated JAK/STAT signals, resulting in transcriptional activation of *PD-L1*. (Fig. 6) The interplay between IL-10 and cAMP/PDE4 has been recognized before^{2, 42}, and linking them to PD-L1 expression expands the portfolio of immune-suppressive activities that are cAMP-driven and IL-10

executed. Conversely, considering the mainly pro-inflammatory role of IL-6, its cAMP-mediated transcription/secretion is less intuitive. This apparent contradiction may be in part explained by the context-dependency of cAMP effects. For example, while cAMP dampens LPS-mediated IL-6 induction in cells of the innate immune system, it can also directly promote *IL-6* transcription/secretion^{43–45}, as we detected in our models. IL-8 is a chemokine produced by monocytes, neutrophils, fibroblasts and tumor cells, which plays an important role within the tumor microenvironment as a chemotactic factor⁴⁶. This expression pattern explains the more restricted effects of cAMP on *IL-8* transcription/secretion, which in our examination was limited to cancer cells. Analogous to the IL-6 paradigm, despite its primarily pro-inflammatory role⁴⁶, we found that IL-8 readily induces PD-L1 in DLBCL, in agreement with earlier reports in gastric cancer⁴⁷. However, contrary to IL-6, the link between cAMP and IL-8 expression is likely to be indirect and may involve IL-1 (as preliminarily shown in Fig. 4A), a cAMP-induced cytokine that transcriptionally activates IL-8^{48, 49}. Interestingly, very recently, systemic and tumor-associated IL-8 was identified as modulator of the cellular profile of the tumor microenvironment, and associated with poor response to immune checkpoint blockade^{50, 51}. It is possible that the cytokines involved as intermediaries in the cAMP-PD-L1 interplay will vary according to the tissue type. However, encouragingly, we also found a significant correlation between *PD-L1* and *IL-10*, *IL-8*, *IL-6* expression in melanoma, lung and colon cancer. Together, we proposed that, at least in a B-cell tumor model, there is a cytokine hierarchy at the intersection of cAMP production and PD-L1 expression, wherein the immunosuppressive IL-10 plays a dominant role, while IL-6 and IL-8 contribute, possibly as a part of feedback negative loop to limit their own pro-inflammatory effects.

We developed part of our data in DLBCL cell lines and in the ex vivo analysis of PDX models. This aspect of the work provided an opportunity to add mechanistic understanding to the known association between PD-L1 expression and ABC-DLBCL (non-GCB DLBCL), which contrasts with a low/null PD-L1 levels in GCB-DLBCL^{52, 53}. While cAMP levels and PKA activity were equally inducible in ABC-like and GCB-like DLBCL cell lines, as we reviewed earlier¹², in the latter the expression/secretion of cytokines was not elicited. This blockade prevented the establishment of the autocrine loop identified in ABC-DLBCLs and, as a result, cAMP did not activate JAK/STAT or induced PD-L1 expression in GCB DLBCLs. Notably, bypassing the cAMP-signaling network with the potent PD-L1 regulator IFN γ also did not induce PD-L1 expression in the GCB models, although in this instance STAT was readily engaged. Thus, in respect to induction of PD-L1 expression in GCB-DLBCL, at least two regulatory nodes appear to be deficient: a) cytokine expression and engagement of the autocrine loop and, b) the activation of the PD-L1 promoter by phosphorylated STATs. These findings point to a putative architectural/functional silencing of cytokines and PD-L1 promoters in the GCB-DLBCL, which may reflect the B-cell developmental stage from which these tumors derive, i.e., their cell of origin. These observations are relevant because they challenge a current paradigm, in which it is implied that since GCB-DLBCLs often display a “non-inflamed” immune environment, the lack of PD-L1 expression in the lymphoma cell would be secondary to the absence of local stimuli⁵². Indeed, as our data were generated in cell lines and thus without the confounding immune microenvironment, we could establish that lymphoma cell-intrinsic defects are at

least partially responsible for the low/null PD-L1 expression in subsets of DLBCL. Nonetheless, it is important to highlight that irrespective of the molecular subtype, DLBCL display very low overall response to checkpoint inhibitors^{52, 54}. In addition, the interplay between cAMP/PDE4 and PD-L1 expression that we describe herein, is unlikely to play a dominant role in this lack of response.

PDE4 inhibitors, which are FDA-approved for COPD and psoriatic arthritis, elevate cAMP levels in cells on the innate and adaptive immune system, and display broad immunosuppressive properties, which we showed may at least part be due to PD-L1 expression. Although increase in PD-L1 levels in tumor cells has been considered a desired biomarker for checkpoint inhibitors activity^{13–15, 52}, this concept needs to be contextualized and, herein, our postulate was that the output of PDE4 inhibition, with the potential to suppress cytotoxic secretion and the immune microenvironment, could in fact associate poor response to immune checkpoint blockade. Remarkably, roflumilast did not decrease the anti-lymphoma activity of an anti-PD-L1 antibody, but this “neutral” outcome was achieved in unexpected ways. The efficacy of anti-PD-L1 used as single agent was, predictably, associated with a substantial T-cell infiltrate in the tumor microenvironment. Conversely, although the anti-lymphoma efficacy of the roflumilast/anti-PD-L1 combination was not significantly inferior to anti-PD-L1 alone, the T-cell infiltrate was quantitatively modest and instead displayed a subtle, and potentially consequential, qualitative changes, including an increase in CD8 cytotoxic T-cells and decrease in CD4 T-cells. Certainly, the changes in the TIL profile mediated by PDE4 inhibition are not sufficient to promote anti-tumor immunity, as roflumilast was ineffective as a single agent. However, they may explain how even in absence of a prominent T-cell infiltrate, the roflumilast/anti-PD-L1 combination still maintained anti-cancer activity. In the future, it would be important to expand these observations and better characterize the subpopulation of TILs, as well as define the role of cAMP signals on macrophages, natural killer and myeloid-derived suppressor cells, as they all play a part on the response to checkpoint blockade. In extrapolating our finding to the clinical realm, two observations may be pertinent: 1) COPD patients, who are prescribed roflumilast “on label”, are at a significantly higher risk for lung cancer. Yet, data from the three pivotal roflumilast trials, which include more than 9000 patients^{16–18}, did not show an increase in cancer diagnosis, even though cAMP is immunosuppressive and could compromise natural anti-cancer immunity. This observation may reflect the qualitative changes in the tumor infiltrate that we described, which could offset the overall immunosuppression. 2) Strategies to establish a *de novo* inflamed tumor microenvironment, which could improve therapeutic responses to checkpoint inhibitors are highly sought. In these models, PD-L1 expression in tumor cells is a regulatory counter response to T-cell activity and is mediated in large part by IFN γ . Although somewhat paradoxically, given its anti-inflammatory role, we speculate that PDE4 inhibitors may have a role to play in these approaches, as it could: a) sustain PD-L1 expression independent of IFN γ signals via traditionally suppressive cytokines, i.e., IL-10, b) it could limit undesirable systemic inflammatory responses and, c) it could establish a favorable local anti-tumor immune profile, as we found in the A20 model.

In summary, the data reported here expand the understanding of the mechanistic basis of cAMP-mediated immunosuppression, by defining the existence of a hitherto unappreciated

interplay with the PD-1/PD-L1 immune checkpoint axis (Fig. 6). These observations may help guide the clinical usage of FDA-approved PDE4 inhibitors.

Supplementary Material

Refer to Web version on PubMed Central for supplementary material.

Acknowledgements:

R.C.T.A. was supported by RP150277, RP170146 (Cancer Prevention and Research Institute of Texas), TRP 6524-17(Leukemia and Lymphoma Society), R01ES031522 (NIEHS/NIH) and I01BX001882 (Veterans Administration Merit Award). The FACS core facility is supported by P30 CA054174 (NCI/NIH).

References:

1. Sassone-Corsi P The cyclic AMP pathway. *Cold Spring Harb Perspect Biol* 2012 12; 4(12).
2. Raker VK, Becker C, Steinbrink K. The cAMP Pathway as Therapeutic Target in Autoimmune and Inflammatory Diseases. *Front Immunol* 2016; 7: 123. [PubMed: 27065076]
3. Serezani CH, Ballinger MN, Aronoff DM, Peters-Golden M. Cyclic AMP: master regulator of innate immune cell function. *Am J Respir Cell Mol Biol* 2008 8; 39(2): 127–132. [PubMed: 18323530]
4. Mosenden R, Tasken K. Cyclic AMP-mediated immune regulation--overview of mechanisms of action in T cells. *Cell Signal* 2011 6; 23(6): 1009–1016. [PubMed: 21130867]
5. Cooney JD, Lin AP, Jiang D, Wang L, Suhasini AN, Myers J, et al. Synergistic Targeting of the Regulatory and Catalytic Subunits of PI3Kdelta in Mature B-cell Malignancies. *Clinical cancer research : an official journal of the American Association for Cancer Research* 2018 3 1; 24(5): 1103–1113. [PubMed: 29246942]
6. Kim SW, Rai D, Aguiar RC. Gene set enrichment analysis unveils the mechanism for the phosphodiesterase 4B control of glucocorticoid response in B-cell lymphoma. *Clinical cancer research : an official journal of the American Association for Cancer Research* 2011 11 1; 17(21): 6723–6732. [PubMed: 21742807]
7. Kim SW, Rai D, McKeller MR, Aguiar RC. Rational combined targeting of phosphodiesterase 4B and SYK in DLBCL. *Blood* 2009 6 11; 113(24): 6153–6160. [PubMed: 19369227]
8. Smith PG, Wang F, Wilkinson KN, Savage KJ, Klein U, Neuberg DS, et al. The phosphodiesterase PDE4B limits cAMP-associated PI3K/AKT-dependent apoptosis in diffuse large B-cell lymphoma. *Blood* 2005 1 1; 105(1): 308–316. [PubMed: 15331441]
9. Conti M, Richter W, Mehats C, Livera G, Park JY, Jin C. Cyclic AMP-specific PDE4 phosphodiesterases as critical components of cyclic AMP signaling. *J Biol Chem* 2003 2 21; 278(8): 5493–5496. [PubMed: 12493749]
10. Kelly K, Mejia A, Suhasini AN, Lin AP, Kuhn J, Karnad AB, et al. Safety and Pharmacodynamics of the PDE4 Inhibitor Roflumilast in Advanced B-cell Malignancies. *Clinical cancer research : an official journal of the American Association for Cancer Research* 2017 3 01; 23(5): 1186–1192. [PubMed: 27542768]
11. Butler MJ, Aguiar RCT. Biology Informs Treatment Choices in Diffuse Large B Cell Lymphoma. *Trends in cancer* 2017 12; 3(12): 871–882. [PubMed: 29198442]
12. Cooney JD, Aguiar RC. Phosphodiesterase 4 inhibitors have wide-ranging activity in B-cell malignancies. *Blood* 2016 12 22; 128(25): 2886–2890. [PubMed: 27756749]
13. Pardoll DM. The blockade of immune checkpoints in cancer immunotherapy. *Nat Rev Cancer* 2012 3 22; 12(4): 252–264. [PubMed: 22437870]
14. Prestipino A, Zeiser R. Clinical implications of tumor-intrinsic mechanisms regulating PD-L1. *Science translational medicine* 2019 2 6; 11(478).
15. Cha JH, Chan LC, Li CW, Hsu JL, Hung MC. Mechanisms Controlling PD-L1 Expression in Cancer. *Mol Cell* 2019 11 7; 76(3): 359–370. [PubMed: 31668929]

16. Rabe KF, Bateman ED, O'Donnell D, Witte S, Bredenbroker D, Bethke TD. Roflumilast--an oral anti-inflammatory treatment for chronic obstructive pulmonary disease: a randomised controlled trial. *Lancet* 2005 8 13–19; 366(9485): 563–571. [PubMed: 16099292]
17. Calverley PMA, Rabe KF, Goehring U-M, Kristiansen S, Fabbri LM, Martinez FJ, et al. Roflumilast in symptomatic chronic obstructive pulmonary disease: two randomised clinical trials. *Lancet (London, England)* 2009 8 29; 374(9691): 685–694.
18. Fabbri LM, Calverley PM, Izquierdo-Alonso JL, Bundschuh DS, Brose M, Martinez FJ, et al. Roflumilast in moderate-to-severe chronic obstructive pulmonary disease treated with longacting bronchodilators: two randomised clinical trials. *Lancet* 2009 8 29; 374(9691): 695–703. [PubMed: 19716961]
19. Wedzicha JA, Calverley PM, Rabe KF. Roflumilast: a review of its use in the treatment of COPD. *Int J Chron Obstruct Pulmon Dis* 2016; 11: 81–90. [PubMed: 26792988]
20. Papp K, Cather JC, Rosoph L, Sofen H, Langley RG, Matheson RT, et al. Efficacy of apremilast in the treatment of moderate to severe psoriasis: a randomised controlled trial. *Lancet (London, England)* 2012 8 25; 380(9843): 738–746.
21. Schafer P Apremilast mechanism of action and application to psoriasis and psoriatic arthritis. *Biochem Pharmacol* 2012 6 15; 83(12): 1583–1590. [PubMed: 22257911]
22. Schett G Apremilast in psoriatic arthritis. *Clinical and experimental rheumatology* 2015 Sep-Oct; 33(5 Suppl 93): S98–100.
23. Bouamar H, Abbas S, Lin AP, Wang L, Jiang D, Holder KN, et al. A capture-sequencing strategy identifies IRF8, EBF1, and APRIL as novel IGH fusion partners in B-cell lymphoma. *Blood* 2013 8 1; 122(5): 726–733. [PubMed: 23775715]
24. Townsend EC, Murakami MA, Christodoulou A, Christie AL, Koster J, DeSouza TA, et al. The Public Repository of Xenografts Enables Discovery and Randomized Phase II-like Trials in Mice. *Cancer Cell* 2016 7 11; 30(1): 183.
25. Lin AP, Abbas S, Kim SW, Ortega M, Bouamar H, Escobedo Y, et al. D2HGDH regulates alpha-ketoglutarate levels and dioxygenase function by modulating IDH2. *Nature communications* 2015; 6: 7768.
26. Suhasini AN, Wang L, Holder KN, Lin AP, Bhatnagar H, Kim SW, et al. A phosphodiesterase 4B-dependent interplay between tumor cells and the microenvironment regulates angiogenesis in B-cell lymphoma. *Leukemia* 2016 3; 30(3): 617–626. [PubMed: 26503641]
27. Rai D, Kim SW, McKeller MR, Dahia PL, Aguiar RC. Targeting of SMAD5 links microRNA-155 to the TGF-beta pathway and lymphomagenesis. *Proc Natl Acad Sci U S A* 2010 2 16; 107(7): 3111–3116. [PubMed: 20133617]
28. Bouamar H, Jiang D, Wang L, Lin AP, Ortega M, Aguiar RC. MicroRNA 155 Control of p53 Activity Is Context Dependent and Mediated by Aicda and Socs1. *Mol Cell Biol* 2015 4 15; 35(8): 1329–1340. [PubMed: 25645925]
29. Ortega M, Bhatnagar H, Lin AP, Wang L, Aster JC, Sill H, et al. A microRNA-mediated regulatory loop modulates NOTCH and MYC oncogenic signals in B- and T-cell malignancies. *Leukemia* 2015 4; 29(4): 968–976. [PubMed: 25311243]
30. Jiang D, Aguiar RC. MicroRNA-155 controls RB phosphorylation in normal and malignant B lymphocytes via the noncanonical TGF-beta1/SMAD5 signaling module. *Blood* 2014 1 2; 123(1): 86–93. [PubMed: 24136167]
31. Elkashef SM, Lin AP, Myers J, Sill H, Jiang D, Dahia PLM, et al. IDH Mutation, Competitive Inhibition of FTO, and RNA Methylation. *Cancer cell* 2017 5 08; 31(5): 619–620. [PubMed: 28486104]
32. Li C, Kim SW, Rai D, Bolla AR, Adhvaryu S, Kinney MC, et al. Copy number abnormalities, MYC activity, and the genetic fingerprint of normal B cells mechanistically define the microRNA profile of diffuse large B-cell lymphoma. *Blood* 2009 6 25; 113(26): 6681–6690. [PubMed: 19278952]
33. Jung I, Aguiar RC. MicroRNA-155 expression and outcome in diffuse large B-cell lymphoma. *Br J Haematol* 2009 1; 144(1): 138–140. [PubMed: 19016736]

34. Coelho MA, de Carne Trecesson S, Rana S, Zecchin D, Moore C, Molina-Arcas M, et al. Oncogenic RAS Signaling Promotes Tumor Immuno-resistance by Stabilizing PD-L1 mRNA. *Immunity* 2017 12 19; 47(6): 1083–1099 e1086. [PubMed: 29246442]
35. Qiu Z, Lin AP, Jiang S, Elkashef SM, Myers J, Srikantan S, et al. MYC Regulation of D2HGDH and L2HGDH Influences the Epigenome and Epitranscriptome. *Cell Chem Biol* 2020 2 24.
36. Manning CD, Burman M, Christensen SB, Cieslinski LB, Essayan DM, Grous M, et al. Suppression of human inflammatory cell function by subtype-selective PDE4 inhibitors correlates with inhibition of PDE4A and PDE4B. *Br J Pharmacol* 1999 12; 128(7): 1393–1398. [PubMed: 10602317]
37. Gantner F, Gotz C, Gekeler V, Schudt C, Wendel A, Hatzelmann A. Phosphodiesterase profile of human B lymphocytes from normal and atopic donors and the effects of PDE inhibition on B cell proliferation. *Br J Pharmacol* 1998 3; 123(6): 1031–1038. [PubMed: 9559883]
38. Sandelin A, Wasserman WW, Lenhard B. ConSite: web-based prediction of regulatory elements using cross-species comparison. *Nucleic Acids Res* 2004 7 1; 32(Web Server issue): W249–252. [PubMed: 15215389]
39. Prestipino A, Emhardt AJ, Aumann K, O’Sullivan D, Gorantla SP, Duquesne S, et al. Oncogenic JAK2(V617F) causes PD-L1 expression, mediating immune escape in myeloproliferative neoplasms. *Science translational medicine* 2018 2 21; 10(429).
40. Sagiv-Barfi I, Kohrt HE, Czerwinski DK, Ng PP, Chang BY, Levy R. Therapeutic antitumor immunity by checkpoint blockade is enhanced by ibrutinib, an inhibitor of both BTK and ITK. *Proc Natl Acad Sci U S A* 2015 3 3; 112(9): E966–972. [PubMed: 25730880]
41. Idos GE, Kwok J, Bonthala N, Kysh L, Gruber SB, Qu C. The Prognostic Implications of Tumor Infiltrating Lymphocytes in Colorectal Cancer: A Systematic Review and Meta-Analysis. *Sci Rep* 2020 2 25; 10(1): 3360. [PubMed: 32099066]
42. Liopeta K, Boubali S, Virgilio L, Thyphronitis G, Mavrothalassitis G, Dimitracopoulos G, et al. cAMP regulates IL-10 production by normal human T lymphocytes at multiple levels: a potential role for MEF2. *Molecular immunology* 2009 1; 46(3): 345–354. [PubMed: 19058854]
43. Zhang Y, Lin JX, Vilcek J. Synthesis of interleukin 6 (interferon-beta 2/B cell stimulatory factor 2) in human fibroblasts is triggered by an increase in intracellular cyclic AMP. *J Biol Chem* 1988 5 5; 263(13): 6177–6182. [PubMed: 2452159]
44. Szabo-Fresnais N, Blondeau JP, Pomerance M. Activation of the cAMP pathway synergistically increases IL-1-induced IL-6 gene expression in FRTL-5 thyroid cells: involvement of AP-1 transcription factors. *Molecular and cellular endocrinology* 2008 3 12; 284(1–2): 28–37. [PubMed: 18280640]
45. Koga K, Takaesu G, Yoshida R, Nakaya M, Kobayashi T, Kinjyo I, et al. Cyclic adenosine monophosphate suppresses the transcription of proinflammatory cytokines via the phosphorylated c-Fos protein. *Immunity* 2009 3 20; 30(3): 372–383. [PubMed: 19285436]
46. Atta ur R, Harvey K, Siddiqui RA. Interleukin-8: An autocrine inflammatory mediator. *Curr Pharm Des* 1999 4; 5(4): 241–253. [PubMed: 10101223]
47. Sun L, Wang Q, Chen B, Zhao Y, Shen B, Wang H, et al. Gastric cancer mesenchymal stem cells derived IL-8 induces PD-L1 expression in gastric cancer cells via STAT3/mTOR-c-Myc signal axis. *Cell death & disease* 2018 9 11; 9(9): 928. [PubMed: 30206229]
48. Sung SS, Walters JA. Increased cyclic AMP levels enhance IL-1 alpha and IL-1 beta mRNA expression and protein production in human myelomonocytic cell lines and monocytes. *J Clin Invest* 1991 12; 88(6): 1915–1923. [PubMed: 1661292]
49. Kaplanski G, Farnarier C, Kaplanski S, Porat R, Shapiro L, Bongrand P, et al. Interleukin-1 induces interleukin-8 secretion from endothelial cells by a juxtacrine mechanism. *Blood* 1994 12 15; 84(12): 4242–4248. [PubMed: 7994038]
50. Schalper KA, Carleton M, Zhou M, Chen T, Feng Y, Huang SP, et al. Elevated serum interleukin-8 is associated with enhanced intratumor neutrophils and reduced clinical benefit of immune-checkpoint inhibitors. *Nat Med* 2020 5; 26(5): 688–692. [PubMed: 32405062]
51. Yuen KC, Liu LF, Gupta V, Madireddi S, Keerthivasan S, Li C, et al. High systemic and tumor-associated IL-8 correlates with reduced clinical benefit of PD-L1 blockade. *Nat Med* 2020 5; 26(5): 693–698. [PubMed: 32405063]

52. Kline J, Godfrey J, Ansell SM. The immune landscape and response to immune checkpoint blockade therapy in lymphoma. *Blood* 2020 2 20; 135(8): 523–533. [PubMed: 31790142]
53. Kiyasu J, Miyoshi H, Hirata A, Arakawa F, Ichikawa A, Niino D, et al. Expression of programmed cell death ligand 1 is associated with poor overall survival in patients with diffuse large B-cell lymphoma. *Blood* 2015 11 5; 126(19): 2193–2201. [PubMed: 26239088]
54. Ansell SM, Minnema MC, Johnson P, Timmerman JM, Armand P, Shipp MA, et al. Nivolumab for Relapsed/Refractory Diffuse Large B-Cell Lymphoma in Patients Ineligible for or Having Failed Autologous Transplantation: A Single-Arm, Phase II Study. *J Clin Oncol* 2019 2 20; 37(6): 481–489. [PubMed: 30620669]

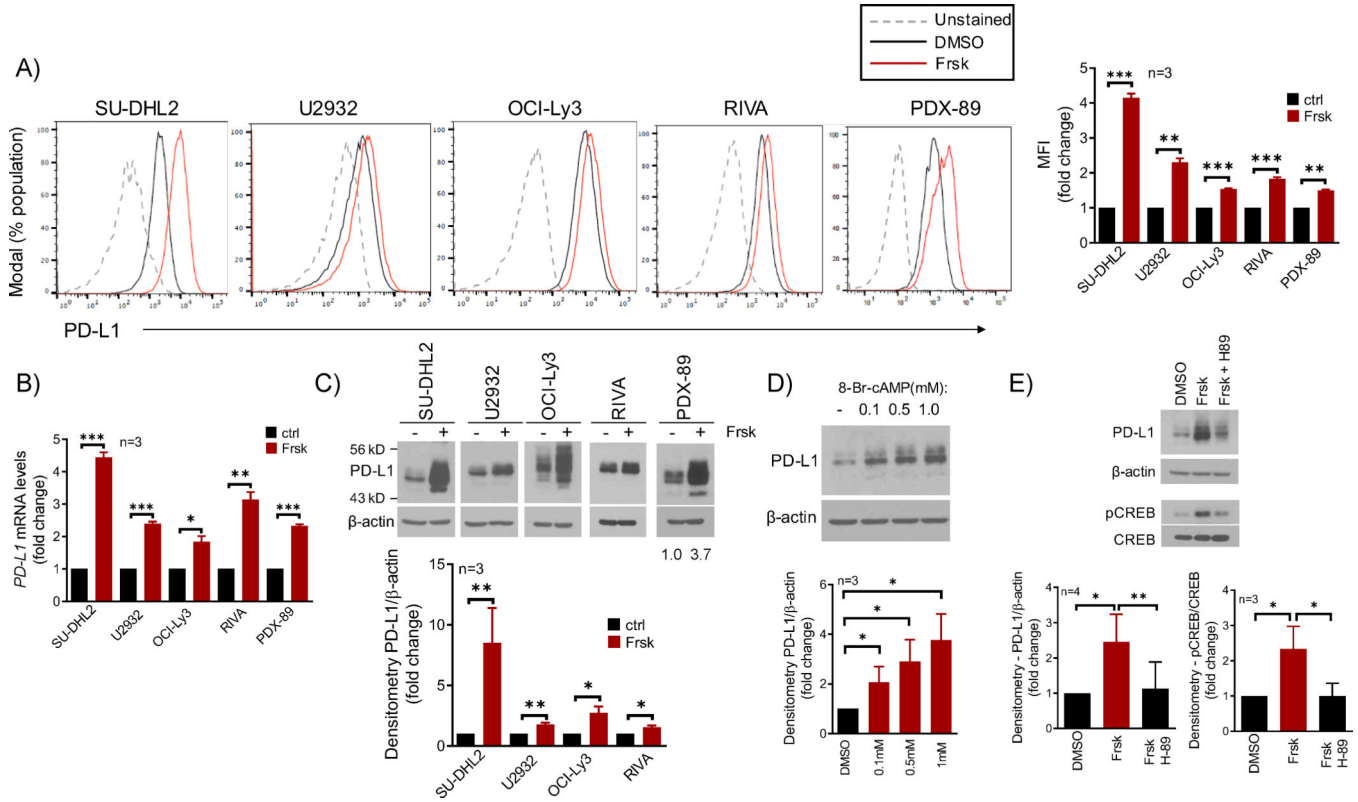


Figure 1. The cAMP/PDE4 axis modulate PD-L1 expression in DLBCL.

A) FACS analysis of cell surface expression of PD-L1 in DLBCL cell line and PDX models in low vs. high cAMP status, DMSO or forskolin (Frsk 20–40 μ M, 16h). Mean fluorescence intensity (MFI) of three replicates is shown in the right panel (full data in Fig. S1B). **B)** q-RT-PCR of *PD-L1* in the same DLBCL cell models in ctrl (DMSO) vs. Frsk (40 μ M, 8–16h). **C)** western blot (WB) analysis of PD-L1 expression in DLBCL models with low vs. high cAMP levels (- and + Frsk, 40 μ M, 16h). Differential baseline PD-L1 expression is shown in Fig. S1G **D)** WB of PD-L1 in the SU-DHL2 cell line exposed to the synthetic cell-permeable 8-bromo-cAMP for 16h. **E)** WB of PD-L1 and phospho-CREB (S133) in the SU-DHL2 cell line exposed to DMSO, forskolin (20 μ M) or forskolin + the PKA inhibitor H-89 (20 μ M) for 4h. In **A)** and **B)**, data shown are mean \pm SD of triplicates. *p<0.05, ** P<0.01, *** p<0.001, two-sided Student's t-test. In **C)**, **D)** and **E)** densitometric quantification of biological replicates is shown below the WBs; data shown are mean \pm SD, p values are from two-sided Student's t-test.

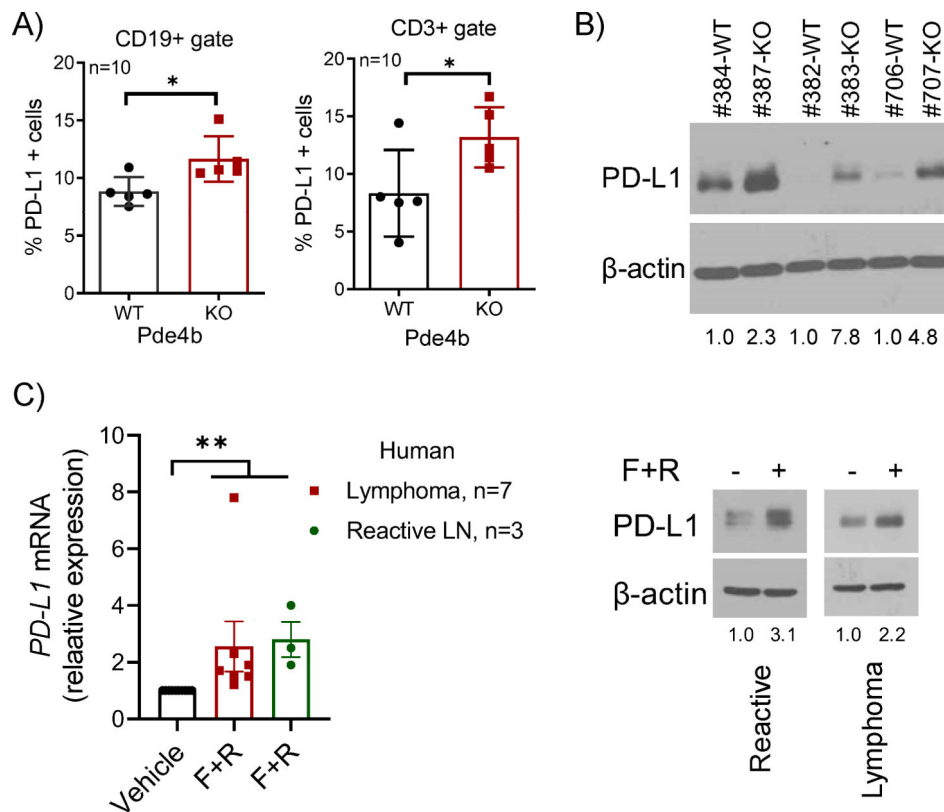


Figure 2. Modulation of PD-L1 expression by the cAMP-PDE4 axis in vivo.

A) FACS analysis of cell-surface PD-L1 expression in splenic B (CD19+) and T (CD3+) cells from Pde4b^{+/+} (WT) and Pde4b^{-/-} (KO) mice (n=10). Data shown are mean \pm SD; p values are from a two-sided Student's t-test, *p<0.05. **B)** WB of PD-L1 in spleen cells of Pde4b KO mice or WT littermates **C) left panel** - Q-RT-PCR-based quantification of *PD-L1* in 10 primary human samples – 3 reactive lymph nodes and 7 mature B cell lymphomas (MCL, MZL, DLBCL, SLL, LPL, FL and CLL) cultured for 8h in presence of vehicle (DMSO) or forskolin (20 μ M) + roflumilast (10 μ M) (F+R); each sample data point represents the mean of quantifications performed in triplicate; data shown are mean \pm SEM; p value was calculated with one-way ANOVA and Tukey's post-test, ** P<0.01; **right panel** - WB of PD-L1 in two representative human primary samples from which enough material was available for protein isolation. Densitometric quantification is shown below the WB in B) and C).

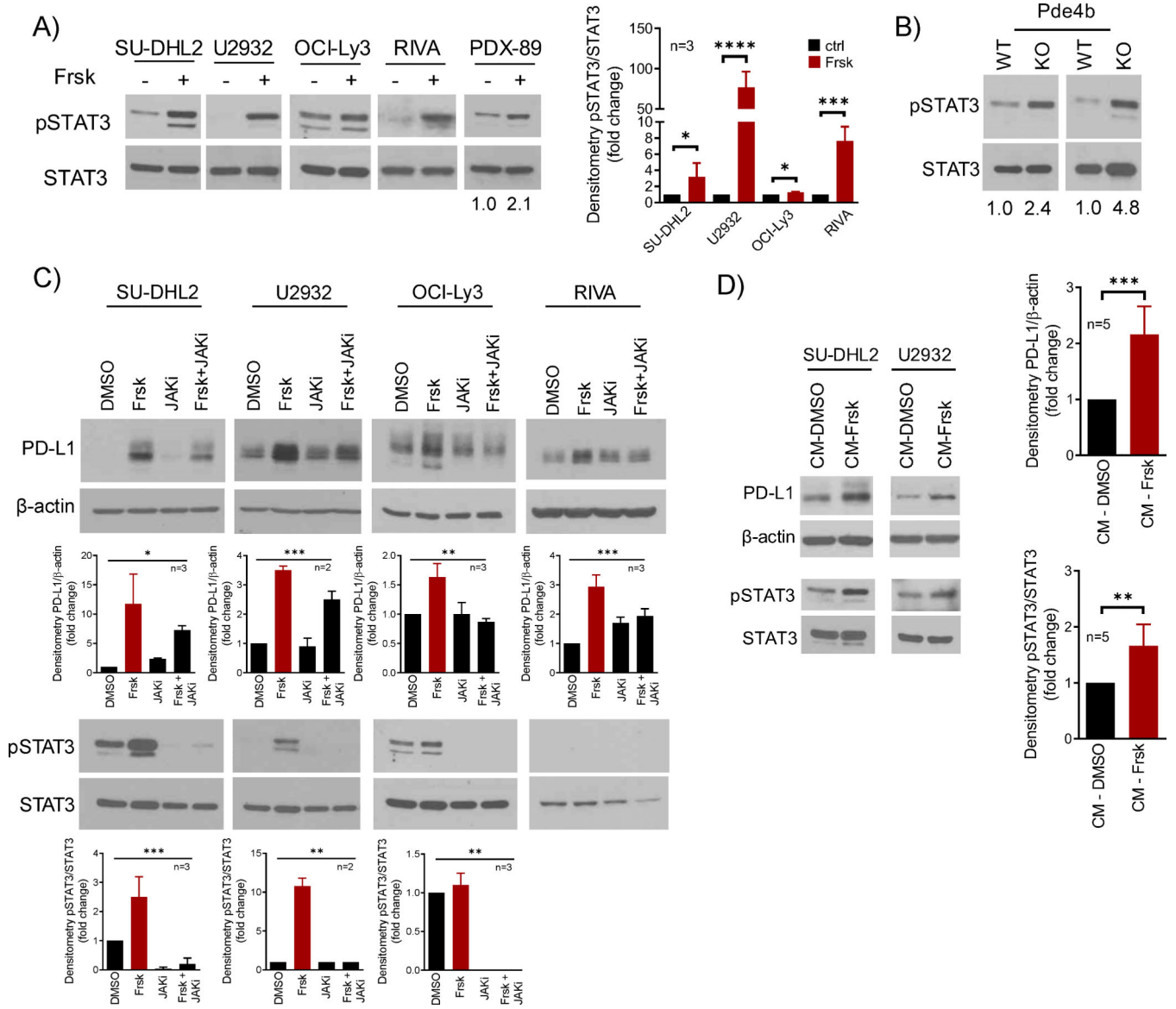


Figure 3. Secreted factors acting on the JAK/STAT signals mediate cAMP induction of PD-L1 expression.

A) WB analysis of pSTAT3 (Y705) and total STAT3 in DLBCL cell lines and PDX model following exposure to forskolin (Frsk, 40µM, 4–16h). The more modest increase in pSTAT3 in OCI-Ly3 reflects the constitutive activity of STAT signals in this cell line - densitometric quantification (pSTAT3/STAT3) of biological replicates is shown on the right, data shown are mean ± SD of replicates, p values are from two-sided Student's t-test. **B)** WB of pSTAT3 (Y705) and total STAT3 in spleen cells of Pde4b KO mice or WT littermates; densitometric quantification (pSTAT3/STAT3) is shown below the WBs. **C)** WB of PD-L1 and pSTAT3 (Y705) in DLBCL cell lines exposed to DMSO, forskolin (Frsk, 40µM), JAKi (JAK inhibitor pyridone 6, 5µM) or their combination for 16h. STAT3 phosphorylation in the RIVA occurs early and it is labile, thus it is detected after 4h exposure to forskolin (panel A), but not after 16h (panel C); the OCI-Ly3 pSTAT3/STAT3 displays in panels A and C are

from the same WB; densitometric quantification is shown below the WBs (PD-L1/ β -actin; pSTAT3/STAT3), data shown are mean \pm SD of biological replicates, p values are from one-way ANOVA. **D)** WB of PD-L1 and pSTAT3 (Y705) in DLBCL cell lines cultured for 8h in conditioned media (CM). The forskolin-free CM was obtained from DLBCL cell lines exposed to DMSO or forskolin (Frsk, 40uM) for 1h, followed by a drug wash-off and replenishment with fresh media. densitometric quantification of biological replicates (n= 5, 3 for DHL2, 2 for U2932) is shown on the right (PD-L1/ β -actin; pSTAT3/STAT3); data are mean \pm SD, p value is from a two-sided Student's t-test.

Author Manuscript

Author Manuscript

Author Manuscript

Author Manuscript

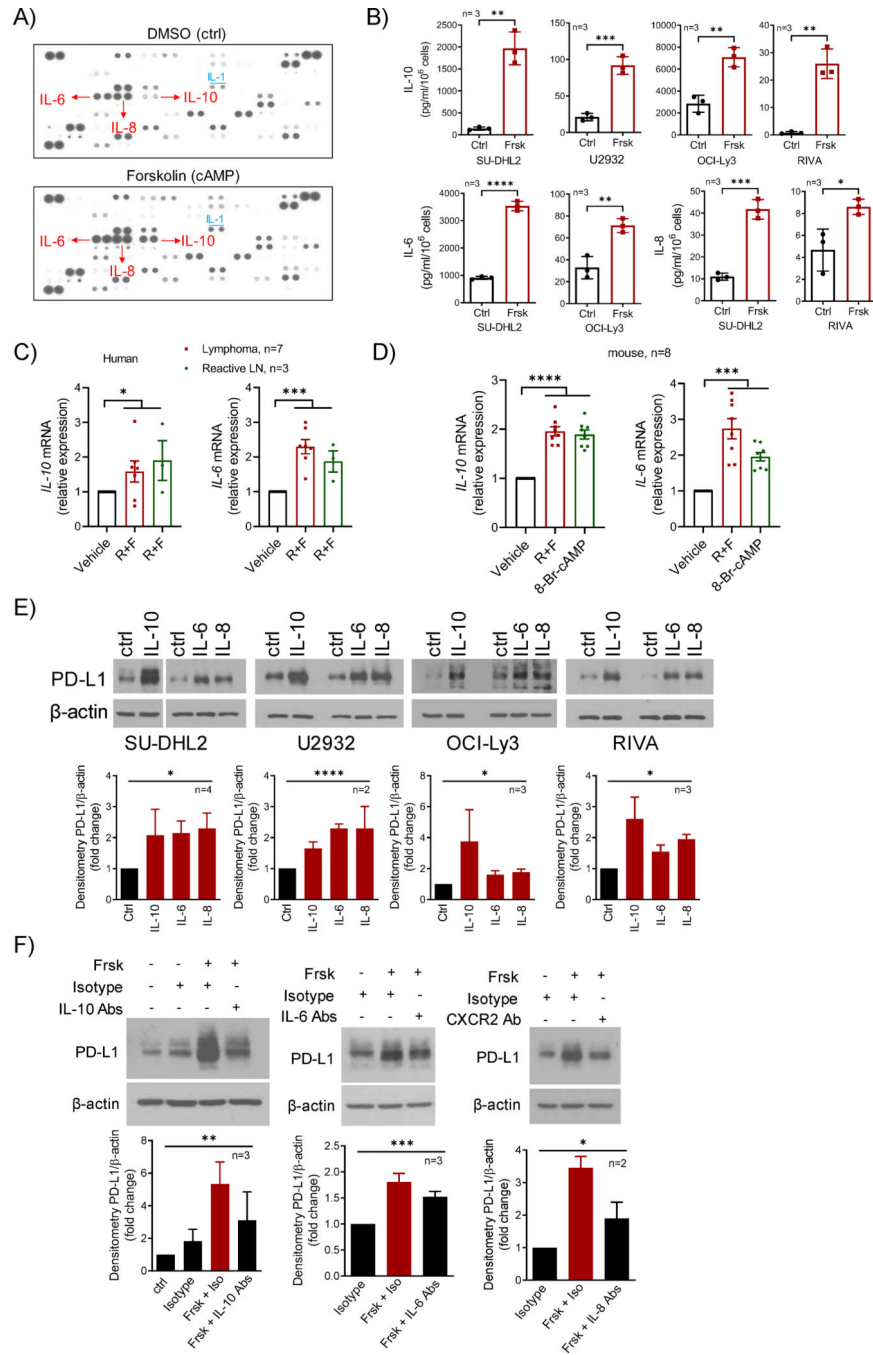


Figure 4. Cyclic-AMP initiates a cytokine executed autocrine loop that promotes PD-L1 expression.

A) Cytokine array exposed to conditioned media from the SU-DHL2 cell line cultured with DMSO (Ctrl) or forskolin (cAMP, 40 μ M) for 8h. Increased levels of IL-6, IL-8, and IL-10 in high cAMP supernatant is indicated by red arrow; increased IL-1 abundance is also noted **B) Top** – ELISA-based quantification of IL-10 in the supernatant of DLBCL cell lines exposed DMSO (Ctrl) or forskolin (Frsk, 40 μ M) for 8h. **Bottom** - ELISA-based quantification of IL-6 and IL-8 in the supernatant of DLBCL cell lines exposed DMSO (Ctrl) or forskolin (Frsk, 40 μ M) for 8h.

(Frsk, 40 μ M) for 8h. **C**) q-RT-PCR quantification of *IL-10* and *IL-6* in primary human reactive lymph nodes or mature B cell tumors cultured for 8h in presence of vehicle (DMSO) or roflumilast (10 μ M) + forskolin (20 μ M), R+F. **D**) q-RT-PCR quantification of *IL-10* and *IL-6* in murine splenocytes cultured for 4h in presence of vehicle (DMSO) or roflumilast (10 μ M) forskolin (40 μ M) (R+F), and 8-Br-cAMP (500 μ M). **E**) WB analysis of PD-L1 in DLBCL cell lines exposed to recombinant IL-10 (10ng/ml), IL-6 or IL-8 (both at 40ng/ml) for 4 to 16h. **F**) WB analysis of PD-L1 in SU-DHL2 cells exposed to forskolin (Frsk, 20 μ M), in the presence of isotypes or anti-IL10 + IL-10 receptor antibodies (5 μ g/each) for 8h (**left panel**), anti-IL6 (10 μ g) + IL-6R (5 μ g) antibodies for 4h (**middle panel**), or anti-CXCR2 antibody (10 μ g) for 4h (**right panel**). Densitometric quantification is shown below the WBs in **E**) and **F**); data shown are mean \pm SD of biological replicates, p values are from one-way ANOVA. In **B**) p values are from two-sided Student's t-test; in **C**) and **D**) each sample data point is the mean of quantifications performed in triplicate and p values are from one-way ANOVA. *p<0.05, ** P<0.01, *** p<0.001, **** p<0.0001.

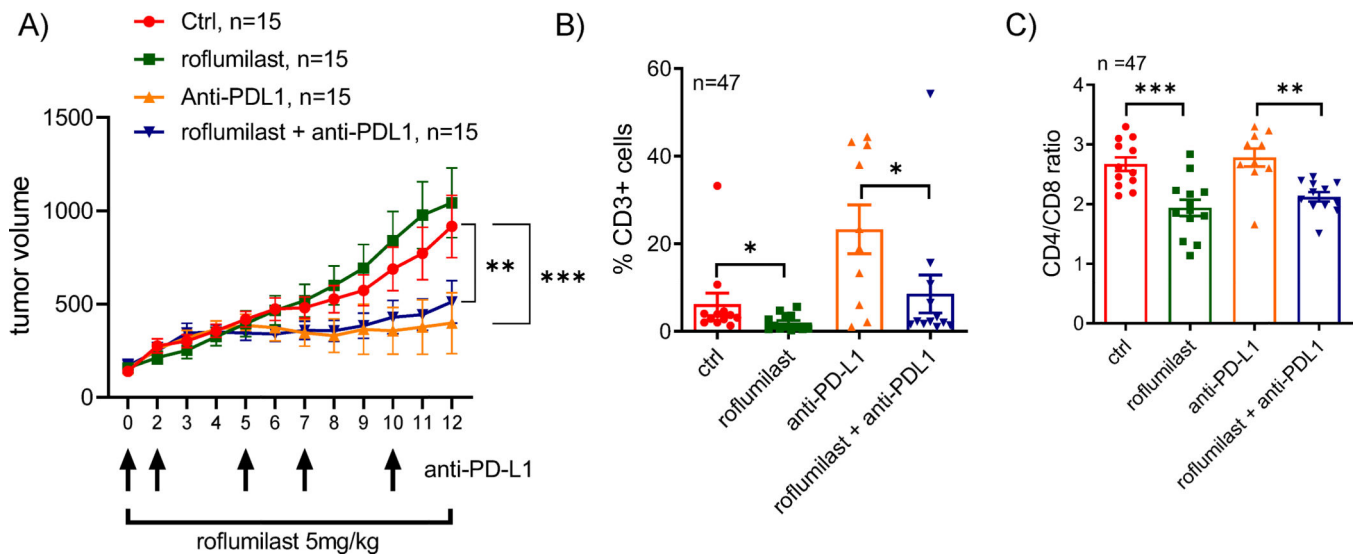


Figure 5. Combination of PDE4 inhibition and checkpoint blockade in a syngeneic murine model of B cell lymphoma.

A) Tumor volume in Balb/c mice engrafted subcutaneously with the A20 lymphoma cells and randomized in four treatment groups (n=60 total, 15/treatment arm). Data are mean \pm SEM, p value is from 2-way ANOVA Tukey's post-test. **B)** FACS analysis of CD3 expression in tumors harvested at the end of the therapeutic trial (n=47). Data shown are mean \pm SEM of the percentage of CD3+ cell in each treatment arm, p value is from two-sided Student's t-test. **C)** Ratio of the percentages of CD4 and CD8 cells determined by FACS in tumors harvested at the end of the therapeutic trial (n=47). Data shown are mean \pm SEM, p value is from two-sided Student's t-test. p<0.05, ** p<0.01, *** p<0.001

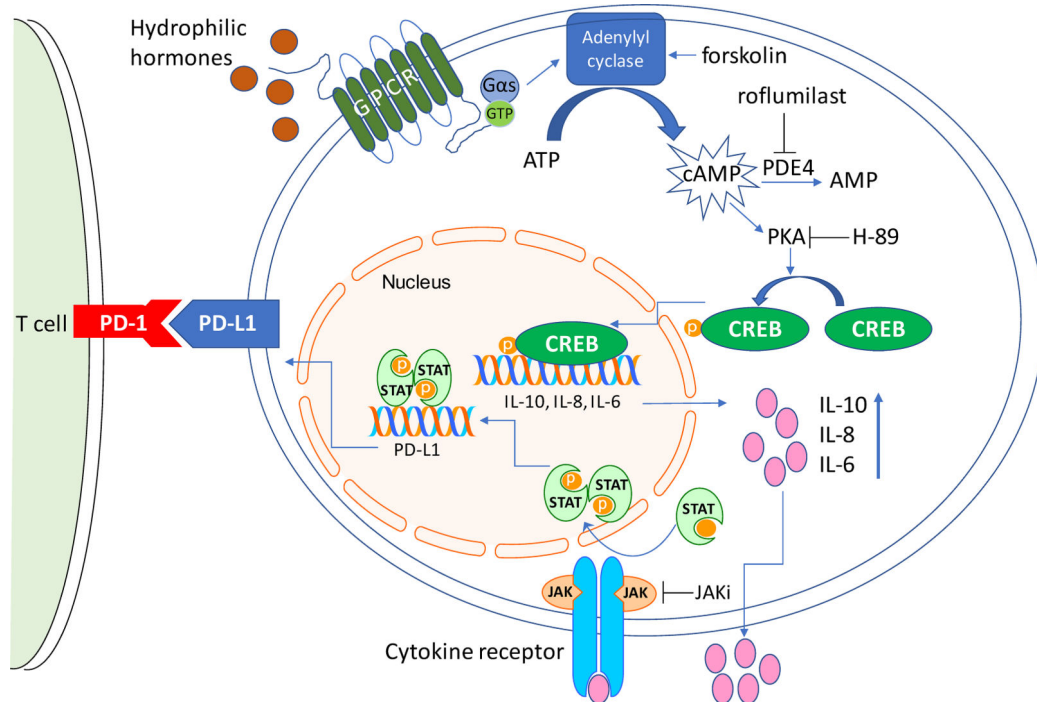


Figure 6. Graphic representation of the signaling axis linking cAMP to PD-L1 expression. Increased intra-cellular levels of cAMP via PKA-CREB transcriptionally activates the *IL-10*, *IL-8* and *IL-6* genes. Secretion of these cytokines engage their receptors in an autocrine fashion, leading to JAK activation and STAT phosphorylation. Phosphorylated STATs bind to and activate the PD-L1 promoter, induce PD-L1 transcription and its cell surface expression. Physiologic stimuli and pharmacological agents that impinge on this pathway are also shown.